Electronic Supplementary Material for:

Graphene oxide-polysulfone filters for tap water purification, obtained by fast microwave oven treatment.

Table of contents:

1. Synthesis

GO was prepared from graphite flakes (Sigma Aldrich, 99% pure, <150 mm) using a modified Hummer's method, as described in Ref. [1]. Further characterization and tests of GO for different applications, including reduction process and biological properties, has been extensively reported in previous works. [2, 3, 4, 5, 6, 7, 8]

Scraps of the industrial production of Polysulfone ultrafiltration membranes (MediSulfone ®) are used as precursor of the granular Polysulfone Hollow Porous Granules (PSU) material.[9]

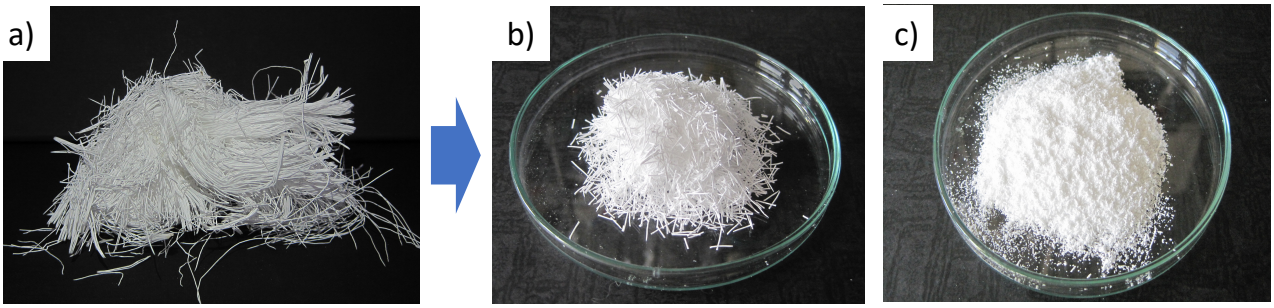

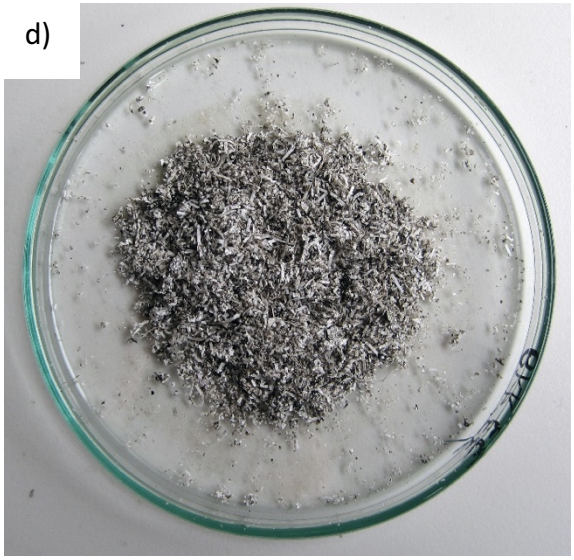

Figure S1. a) Scraps of polysulfone hollow fiber membranes, b) cut scraps and c) grinded scraps (PSU), d) Representative sample PSU-GO-OV.

PSU substrates were prepared by mechanical grinding of polysulfone hollow fiber scraps (figure S1a-c).[9] A final washing of the granules in DI water allows to replace the glycerin introduced during production with the purpose of conserving the fiber structure. The washed material was then placed in a solution of GO in DI water respecting a proportion that allows to have a 5 wt % GO content, i.e. 50 mg of GO (12.5 mL of aqueous solution of GO 4 mg/mL) for 1 gr of PSU-GO. After removal of the

water on a rotary evaporator at 50 °C, the material was treated with focused microwave irradiation. Microwave experiments were carried out at atmospheric pressure with a CEM Discover SP apparatus (f = 2.45 GHz) which has in situ magnetic variable speed, irradiation monitored by PC computer, infrared measurement and continuous feedback temperature control. In a typical experiment, 100 mg of material and 100 μL of DI water in a closed glass vessel (10 ml) were irradiated for 45 min at 100 W (fixed power). The process temperature was stable below 70 °C. The so obtained PSU-GO-MW sample was finally washed in a 1:1 mixture of water/ethanol to remove any traces of unreacted GO and finally left to dry at room temperature to a constant weight.

2. Scanning Electron Microscopy (SEM)

The samples were imaged with a SEM, ZEISS LEO 1530 FEG, operated at 5 kV and secondary electrons were collected by means of an In-Lens detector. Sample were metallized with gold before the measurement. The GO coatings were clearly observed thanks to the edges and ripples typical of 2D materials (Figure S2). The sheets showed good adhesion to the PSU substrate. For comparison, blank PSU-GO composites with no stabilization treatment would instead release large amounts of debris and contaminants when suspended in water, visible by naked eye (Figure S3).

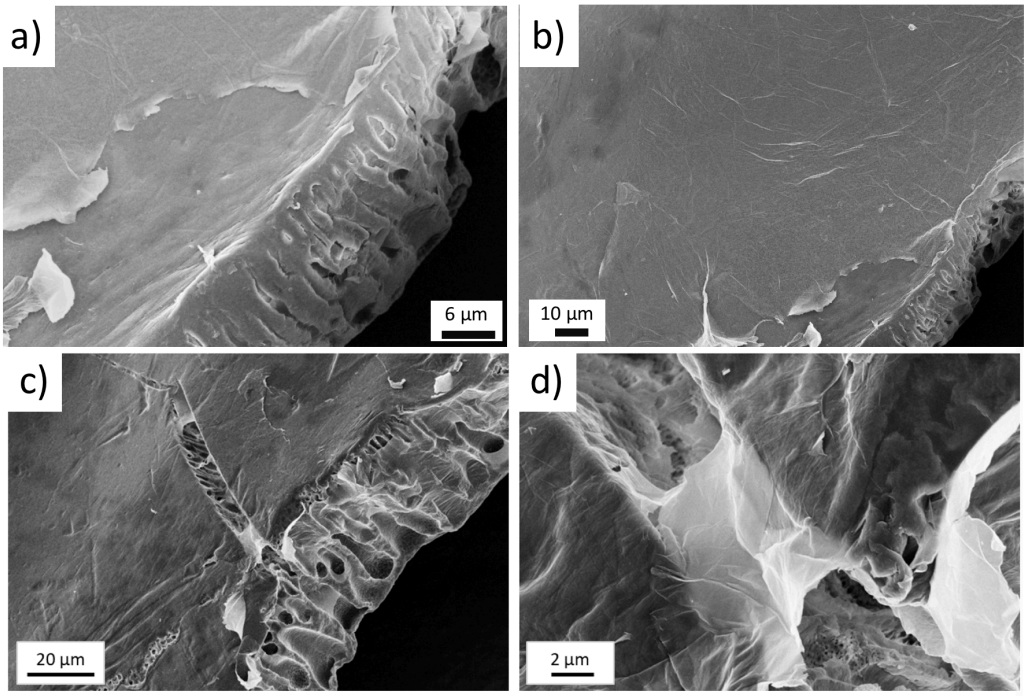

Figure S2. SEM images of different PSU-GO samples. The collected signal is from In-Lens detector. GO is visible when in detached from surfaces of PSU (a), the presence of GO is clearer near the cracks long the PSU granule where GO is suspended (b). SEM images of pure PSU showed a similar microchannel structure of the membrane, but with no presence of 2-dimensional nanosheets.

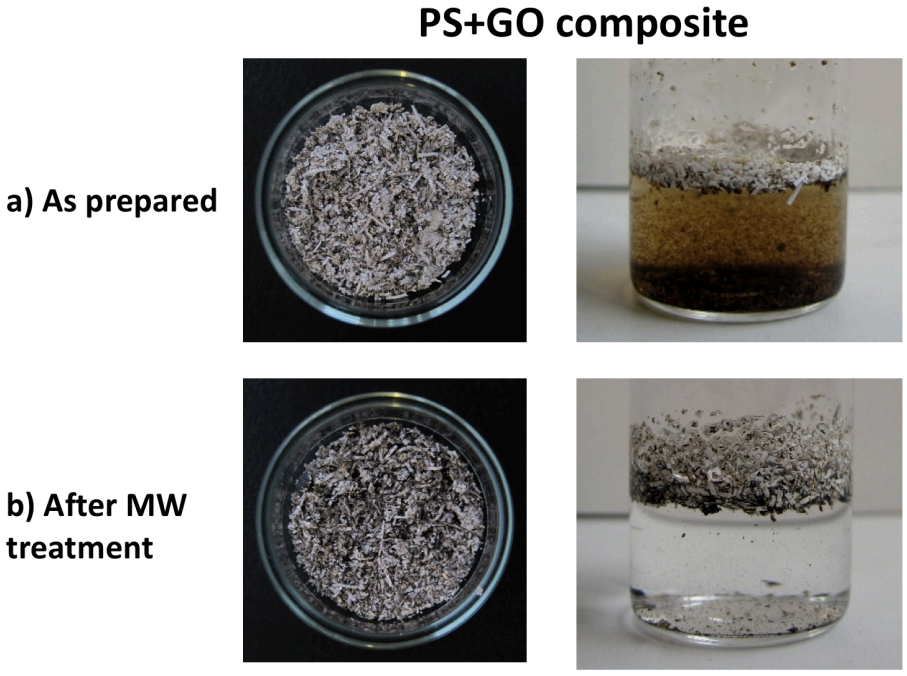

Figure S3. Optical images of dry powders and water dispersions of PSU+GO composite a) as prepared, and b) after stabilizing the GO on PSU by microwaves treatment.

3. X-ray diffraction (XRD)

X-ray diffraction analysis was done with a PANalytical X'Pert PRO powder diffractometer equipped with a fast X'Celerator detector, in Bragg-Brentano geometry. Cu Kα radiation was used (40 mA, 40 kV). The 2-theta range was investigated from 2.50° to 60° with a step size of 0.066° and time/step of 300 s.

Size was estimated with Scherrer equation Crystallite size (average) = k * λ / (B cos θ): k shape factor (=1),[10] [10] λ wavelength (=0.154 nm), B full with at high medium, FWHM, of the considered reflection (instrumental broadening was considered), θ is the diffraction angle of the reflection (=5.85°). The number of GO layers was estimated as ratio of the size and the interlayer distance, obtained from position of (*0 0 1)* GO peak (Table S1).

Table S1. Structural parameters of PSU-GO. Peak position, interlayer distance, width, size, number of GO layers.

Material	d spacing (Å)	size (Å)	# GO layers
Pristine GO	7.8 ± 0.3	109 ± 5	14 ± 1
PSU-GO-MW	8.3 ± 0.3	94 ± 4	11 ± 1
PSU-GO-OV	7.9 ± 0.3	80 ± 4	10 ± 1

4. XPS analysis

Samples were prepared by adding to 1gr of PSU-GO samples about 5 ml of dichloromethane and removing the solvent phase (containing PSU). Four different washing steps were performed per each sample. The XPS spectra were recorded with a Phoibos 100 hemispherical energy analyser (Specs) using Mg Kα radiation (ħω = 1253.6 eV; X-Ray power = 125W) in constant analyser energy (CAE) mode, with analyser pass energies of 10 eV. Base pressure in the analysis chamber during analysis was 310^{-9} mbar. All spectra were calibrated to the C 1s binging energy (285.0 eV). Spectra were fitted by using CasaXPS (www.casaxps.com, figure S4). The O 1s peak was fitted by using a double Voigt curve, while the S 2p doublet with 2 Voigt curves (S 2p3/2 and S 2p1/2) with constrained area ratio (2:1) and spin-orbit split S 2p1/2 - S 2p3/2 = 1.18 eV. The C 1s peak of the pristine PSU was fitted by using the C-C (285.0 eV), C-S (286.3 eV), epoxy C-O-C (286.8 eV) and shake-up at 292.0 eV.[11] [11] C 1s of GO was fitted with aromatic carbon (C-C sp^2, 284.4 eV), aliphatic carbon (C-C sp^3, 285.0 eV), hydroxyl (C-OH, 285.7 eV), epoxy (C-O-C, 286.7 eV), carbonyl (C=O, 288.0

eV) and carboxyl (O-C=O, 289.1 eV), the overall accuracy of the O/C obtained by fit with the O/C obtained from the area ratio of O 1s and C 1s was proved by our previous work.[12] All peak shapes were Voigt, except the aromatic carbon (C-C sp^2), that was fitted with APV (Asymmetric-pseudo Voigt, asymmetry parameter of 0.14).

Table S2 shows the chemical composition of Pristine GO, GO in DCM, and GO obtained from PSU-GO-MW and PSU-GO-OV samples. Figure S4 shows the XPS data of pristine PSU, as reference. The control sample of GO dispersed exposed to DCM showed a negligible variation of the overall oxidation (O/C) and no changes in O-C groups; the relative amount of aromatic and aliphatic carbon sp2/sp3 C-C changed: these 2 peaks are extremely covariant, since they fit (see Figure 2) a single and un-resolved peak in GO signal; thus, only the sum of them can be trusted as an accurate value. A significant change can be observed for the GO treated in oven (PSU-GO-OV samples): the amount of non-oxidised carbon (C-C sp^2 and sp^3) increases up to 58.8 %, C=O and O-C=O groups decrease and the epoxy ring are opened (epoxy C-O-C decreases and hydroxyl C-OH increases), with a decrease of the overall oxidation (O/C=0.30). Conversely, GO obtained from PSU-GO-MW samples has a negligible variation of O/C ratio respect to the pristine GO, only a small variation of epoxy and hydroxyl group compatible with a small fraction of epoxy groups opening.

Table S2. Deconvolution of C 1s peak of GO by different function groups (%) and the obtained O/C ratio.

SAMPLE	C-C sp^2	C-C sp^3	C-OH	C-O-C	C=O	O-C=O	O/C_{fit}
Pristine GO	32.7±0.7	9.5±0.5	2.1±0.2	44.2±0.7	8.2±0.5	3.5±0.4	0.39±0.01
GO in DCM	26.0±0.7	16.5±0.5	2.0±0.2	43.7±0.8	7.2±0.5	4.6±0.4	0.40±0.01
GO-MW*	35.3±0.8	12.5±0.5	4.1±0.4	36.6±0.7	7.8±0.5	3.7±0.4	0.38±0.01
GO-OV*	37.1±0.8	21.7±0.6	8.0±0.5	27.0±0.7	4.1±0.4	2.1±0.2	0.30±0.01

* GO signal obtained after PSU dissolution in DCM. For reference, O/C of blank PSU is 0.13, as obtained from the area ratio of O 1s and C 1s, due to the significant presence of S-O groups in PSU structure.

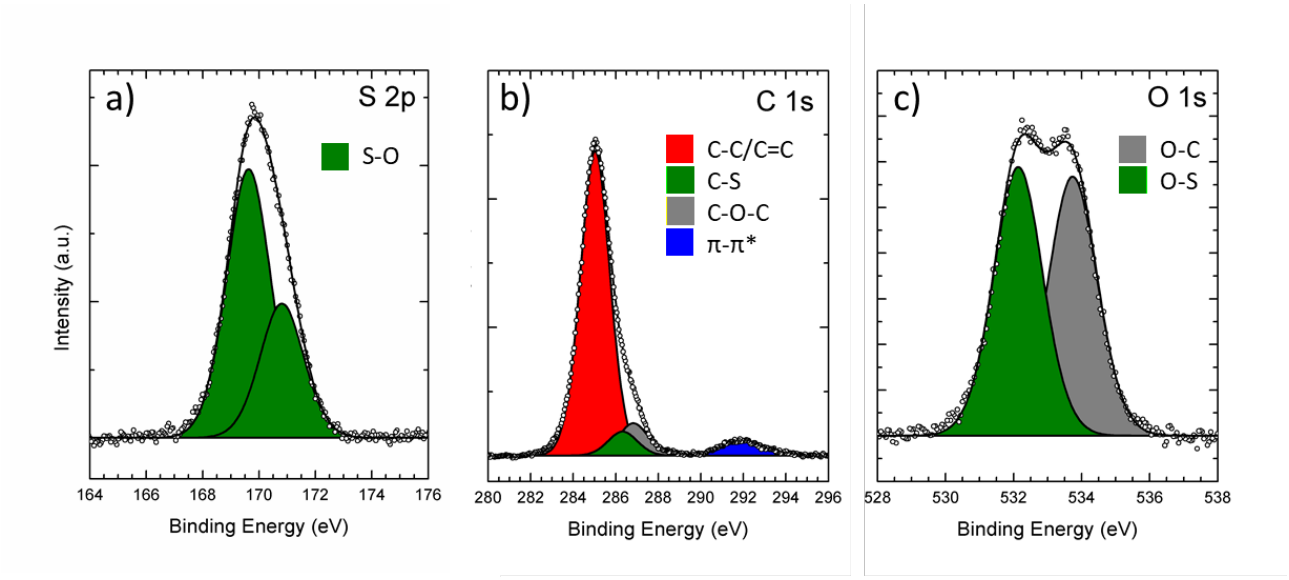

Figure S4. XPS spectra of PSU: a) S 2p, b) C 1s and c) O 1s.

The broadening of C 1s spectrum in PSU-GO is due to the presence of GO: the spectra reported in figure S5 are significantly broader respect to the pristine PSU (Figure S4b) and are similar to the pristine GO C 1s reported in fig 2b. The epoxy group observed at ≈287 eV suggest a GO coverage >50% on the PSU.

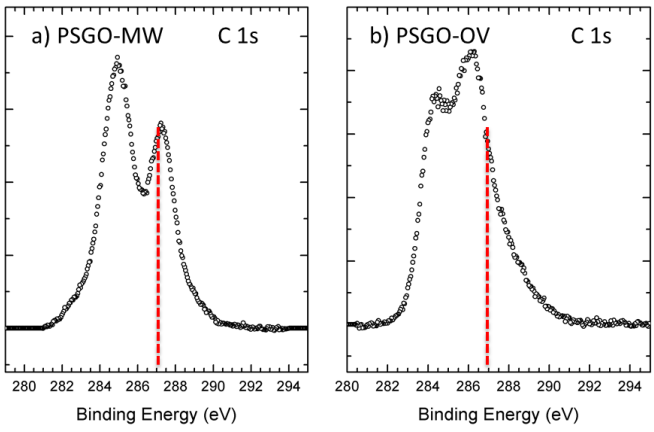

Figure S5. XPS C 1s spectrum of a) PSU-GO-MW and b) PSU-GO-OV. The red dotted line is the approximate position of epoxy group, typically associated to GO.

5. Quantitative measurement of contaminants in solution

High pressure liquid chromatography (HPLC) was performed on an Agilent 1260 HPLC instrument equipped with a diode array detector. 0.5 mL samples were used as sources for the automated injection. The chromatographic separation was performed on a reverse phase Zorbax C8 column 4.6 x 150 mm, 5 μm, with a linear gradient from 0.05% trifluoroacetic acid in water to 100% acetonitrile at flow rate of 1.0 mL/min, detection at λ of maximum UV absorption (296 nm for OFLOX and 540 nm for RhB). Centrifugation at 8000 rpm for 5 min was done prior to the injection. In all experiments, the absorption of each analyte was determined by comparison with that of the initial untreated solution. The analytical samples were kept in the dark and analysed at earliest convenience. The limit of detection was estimated around 50 ng/L for each OFLOX and 5 ng/L for RhB.

6. Adsorption isotherms of GO

The adsorption isotherm of the target contaminants on GO was performed at fixed concentration of RhB and OFLOX by varying the amount of GO. In a total volume of GO suspension (5ml) at different concentration, RhB or OFLOX (in powder, as received) was added. The details of sample preparation are reported in tables S3 and S4. The isotherm curves were obtained equilibrating the solutions for 24 hrs at room temperature. The solutions were analysed by HPLC following the method above reported in section 8.

The isotherms were fitted by Langmuir, BET and Freundlich models. BET adsorption well describes better than other considered models the adsorption of both molecules (the goodness of fit are reported in table S5, S6, S7). OFLOX adsorption could be fitted with BET model, while RhB gave good fit with all models.

Table S3. Experimental parameters of solution used for isotherms of RhB adsorption on GO.

SAMPLE	Volume (mL)	C_0 RhB (mg/mL)	GO (mg)
1	5	1	15
2	5	1	10
3	5	1	5
4	5	1	3
5	5	1	2
6	5	1	1

7	5	0.5	10
8	5	0.5	5
9	5	0.5	3
10	5	0.5	2
11	5	0.5	1

Table S4. Experimental parameters of solution used for isotherms of OFLOX adsorption on GO.

SAMPLE	Volume (mL)	C_0 OFLOXmg/mL)	GO (mg)
1	5	0.8	15
2	5	0.8	10
3	5	0.8	5
4	5	0.8	3
5	5	0.8	2
6	5	0.8	1
7	5	0.5	10
8	5	0.5	5
9	5	0.5	3
10	5	0.5	2
11	5	0.5	1

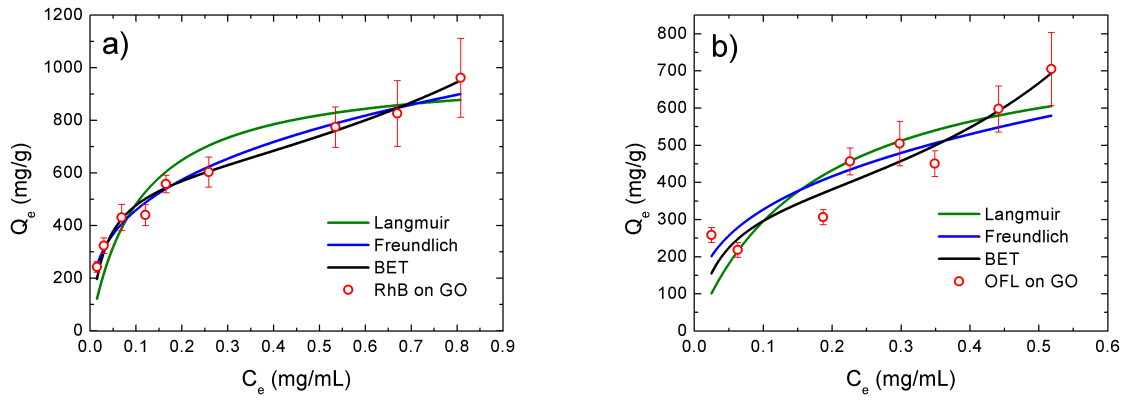

Figure S6. Adsorption isotherms of RhB (a) and OFL (b) on pristine GO, fitted by Langmuir (green line), BET (black line) and Freundlich (blue line) models.

Table S5. Parameter obtained from BET fit of the adsorption isotherms by molecules in liquid phase (Rhodamine and Ofloxacine) on GO.

Adsorbate	Q_m(mg/g)	C_{BET}	Cs	A(m^2/g)	R^2
RhB	588 ± 50	67 ± 10	2.0 ± 0.1	1338 ± 114	0.9935
OFL	356 ± 40	30 ± 5	1.0 ± 0.1	772 ± 87	0.9691

Table S6. Parameter obtained from Langmuir fit of the adsorption isotherms by molecules in liquid phase (Rhodamine and Ofloxacine) on GO.

Adsorbate	Q_m(mg/g)	K_L	R^2
RhB	990 ± 110	9.4 ± 0.9	0.9707
OFL	807 ± 100	5.8 ± 0.7	0.7995

Table S7. Parameter obtained from Freundlich fit of the adsorption isotherms by molecules in liquid phase (Rhodamine and Ofloxacine) on GO.

Adsorbate	K_f(mg/mg·(mL/mg)$^{1/n}$)	1/n	R^2
RhB	0.964 ± 0.080	0.32 ± 0.03	0.9857
OFL	0.728 ± 0.070	0.35 ± 0.03	0.7782

7. Adsorption isotherms of PSU-GO-MW and PSU-GO-OV

The isotherm curves were obtained equilibrating 25 mg of adsorbent in 4 ml of water solution of RhB at concentration ranging from 0.01 to 4 mg/mL and OFLOX at concentration ranging from 0.01 to 2 mg/mL for 24 hrs at room temperature. The isotherms were fitted by Langmuir (eq. 1), BET (eq. 1) and Freundlich models ($Q_e=K_f \cdot C_e^{1/n}$, where the K_f is proportional to adsorption efficiency and 1/n is a constant between 0 and 1). The parameters of different fits are reported in table S8, S9, S10 and Figure S7. BET adsorption describes better than others considered models the adsorption of Ofloxacine molecules. Langmuir model describes better RhB adsorption , even if R^2 of BET and Langmuir are quite similar, thus both models are compatible in principle. Freundlich can be excluded

for both molecules on all substrates. The value of Cs was optimized for each isotherms, in accordance with the BET theory for liquids.[13] [13]

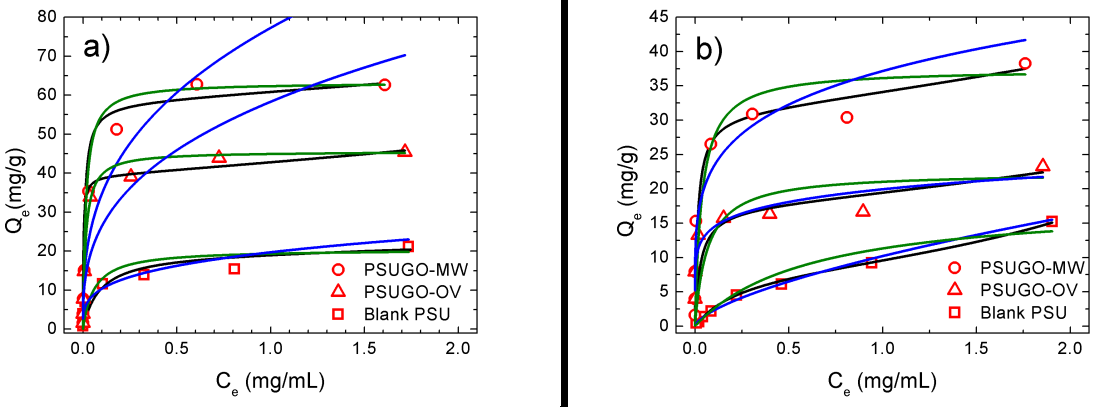

Figure S7. Adsorption isotherms of RhB (a) and OFL (b) on pristine PSU, PSU-GO-MW and PSU-GO-OV, fitted by Langmuir (gre—en line), BET (black line) and Freundlich (blue line) models.

Table S8. Parameter obtained from BET fit of the adsorption isotherms by molecules in liquid phase (Rhodamine B and Ofloxacine) on PSU, PSU-GO-MW and PSU-GO-OV.

Adsorbate	Adsorbent	Q_m(mg/g)	C_{BET}	Cs (mg/mL)	R^2
Rhodamine B	PSU	20 ± 2	230 ± 50	20 ± 1	0.9398
	PSU-GO-MW	58 ± 4	2200 ± 300	20 ± 1	0.9992
	PSU-GO-OV	39 ± 3	4200 ± 500	15 ± 1	0.9993
Ofloxacine	PSU	9 ± 1	17 ± 4	4 ± 1	0.9938
	PSU-GO-MW	31 ± 2	650 ± 80	10 ± 2	0.9969
	PSU-GO-OV	18 ± 1	280 ± 50	8 ± 1	0.9911

Table S9. Parameter obtained from Langmuir fit of the adsorption isotherms by molecules in liquid phase (Rhodamine and Ofloxacine) on PSU, PSU-GO-MW and PSU-GO-OV.

Adsorbate	Adsorbent	Q_m(mg/g)	K_L	R^2
Rhodamine B	PSU	21 ± 2	17 ± 3	0.9730
	PSU-GO-MW	63 ± 4	65 ± 6	0.9995
	PSU-GO-OV	46 ± 3	67 ± 6	0.9995
Ofloxacine	PSU	18 ± 2	2.0 ± 0.5	0.8906
	PSU-GO-MW	37 ± 2	27 ± 3	0.8976
	PSU-GO-OV	22 ± 2	15 ± 2	0.9677

Table S10. Parameter obtained from Freundlich fit of the adsorption isotherms by molecules in liquid phase (Rhodamine and Ofloxacine) on PSU, PSU-GO-MW and PSU-GO-OV.

Adsorbate	Adsorbent	K_f(mg/mg·(mL/mg)$^{1/n}$)	1/n	R^2
Rhodamine B	PSU	0.020 ± 0.004	0.28 ± 0.03	0.9620
	PSU-GO-MW	0.077 ± 0.009	0.35 ± 0.03	0.9216
	PSU-GO-OV	0.058 ± 0.006	0.34 ± 0.03	0.9114
Ofloxacine	PSU	0.010 ± 0.001	0.35 ± 0.03	0.9878
	PSU-GO-MW	0.037 ± 0.005	0.35 ± 0.03	0.9073
	PSU-GO-OV	0.200 ± 0.020	0.14 ± 0.01	0.9099

8. Measurement of surface area by nitrogen gas adsorption

Surface Area was measured with an ASAP 2020 analyser (Micromeritics, USA). Before the analysis the membranes were pre-treated at room temperature for 12 hs under vacuum until stable pressure (10^{-5} mbar). After the treatment, the mass of the samples decreases by 7-10 %, probably due to the removal of adsorbed water. The surface area was measured by using multi-point adsorption data from linear segment of the N_2 adsorption isotherms using Brunauer-Emmett-Teller (BET) theory in according with ASTM D6556 – 10 (table S11).

Table S11. Surface area (m^2/g) of pristine PSU and PSU-GO composites obtained by gas adsorption (N_2) and molecules in liquid phase (Rhodamine and Ofloxacine).

Adsorbent	N_2	Rhodamine B	Ofloxacine
PSU	25.7 ± 0.8	48 ± 5	20 ± 2
PSU-GO-MW	23.6 ± 0.8	143 ± 9	67 ± 4
PSU-GO-OV	24.0 ± 0.8	105 ± 7	39 ± 2

9. XRD and optical comparison after adsorption experiments

Figure S8 shows optical images and XRD patterns of one of the composites (PSU-GO-OV) after exposure to high amounts of RhB. The profile of each sample is dominated by the large bell shaped amorphous halo of PSU polymer centred at 17.6° (2Θ). A low intensity peak is detectable in PSU-GO-OV scan at 11.7° (# layer 12±2): it is due to the GO coating the PSU. After soaking in RhB solution the peak almost disappears, at difference with what observed by similar exposure to pure water. This suggests that Rhodamine B molecules causes disruption of GO regular packing.

The better efficiency of PSU-GO-MW samples for RhB capture respect to pristine PSU was also tested by visual comparison experiments (figure S9).

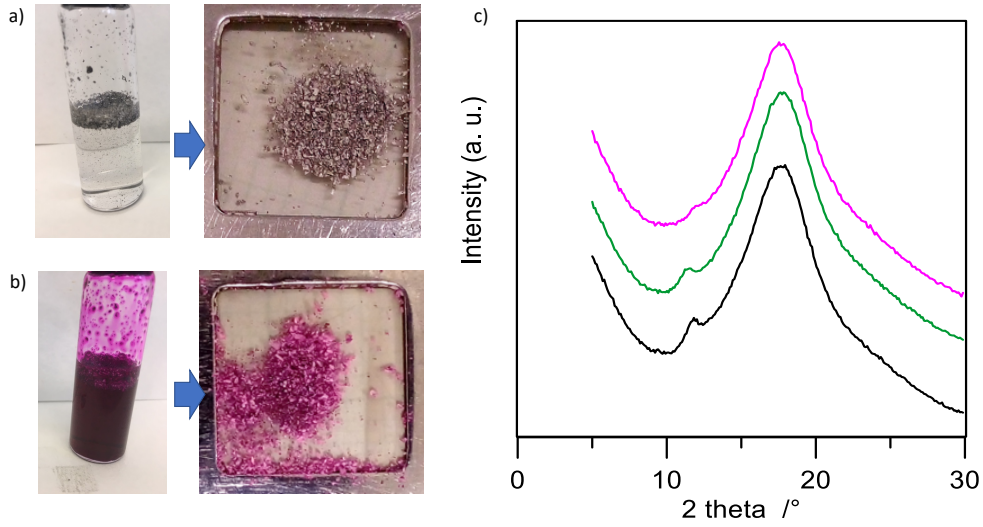

Figure S8. a) PSU-GO-OV after long soaking in water (25mg/4ml, 24hs contact time) b) PSU-GO-OV after long soaking in RhB solution (25mg, RhB 2mg/ml, 4ml 24hs contact time), c) XRD scans of PSU-GO-OV (black); PSU-GO-OV after 24h in mQ water (green, corresponding to the image a), PSU-GO-OV r after 24h in 2 mg/mL RhB solution (magenta, corresponding to the image b).

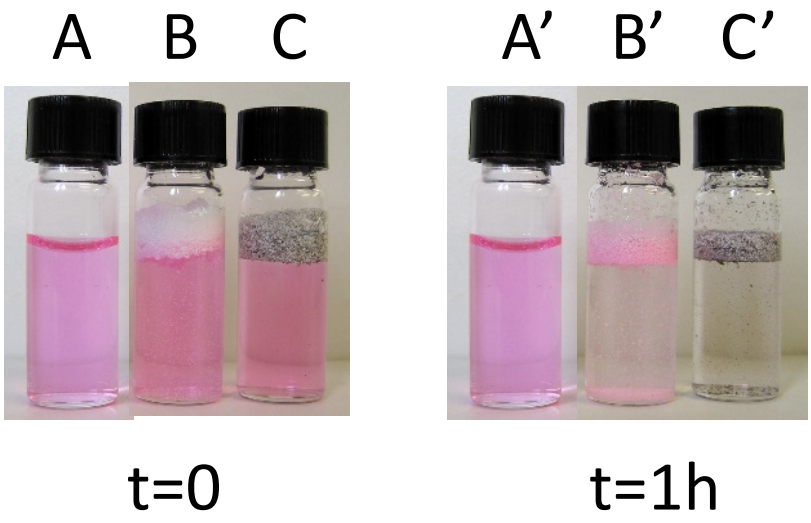

Figure S9. Visual comparison of the removal efficiency of RhB immediately after mixing of after 1 hour. A) Pure Rhodamine 2,5 mg/L, no adsorbent. B) Same as A, but in presence of PS granules. C) Same as, A but in presence of PSU-GO-MW.

10. Aggregation of GO in tap water

We observed in target experiments (figure S10) that GO, while being highly soluble in distilled water, is insoluble in tap water, thus being “intrinsically safe” for this specific application.

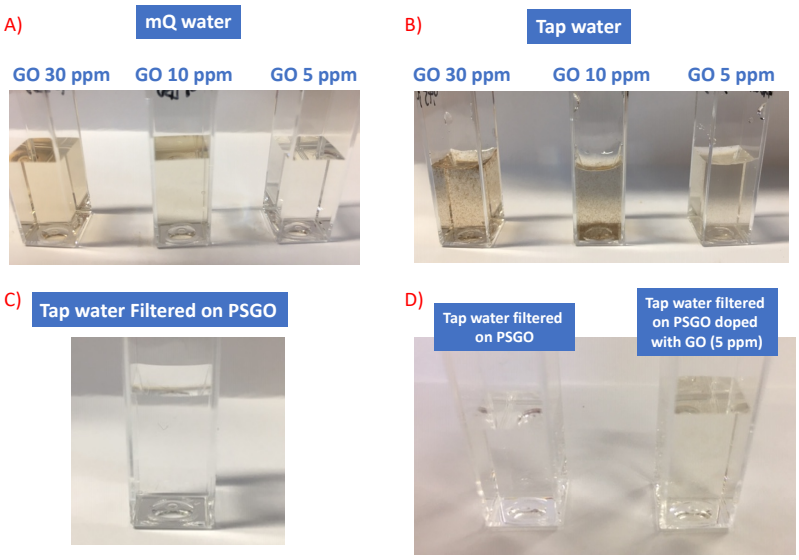

Figure S10. Images of GO suspension in mQ (a) and tap water (b) at different concentrations. precipitation of GO was observed in tap water even at low concentration. c) Sample of water filtered through the cartridge filled with PSU-GO-MW material, showing no GO presence. d) same sample of c) before and after addition of GO (5 ppm), the suspension appears yellow after GO doping and flocculation of GO occurred after about 1h.

11. Release experiments setup

We performed UV-vis spectroscopy on water re-circulated for 100 hours through filters containing PSU-GO-MW and PSU-GO-OV powders (Figure S11, ESI). Detection limit, estimated with calibrated GO solutions, was about 1 ppm.

Figure 5 in main text shows the images of the recirculated water, as well as the UV-vis spectra of the filtered water (red line) and of calibration solutions having a concentration range 0.25-10 ppm. The comparison indicates that any GO possibly released in filtered water was below 1 ppm.

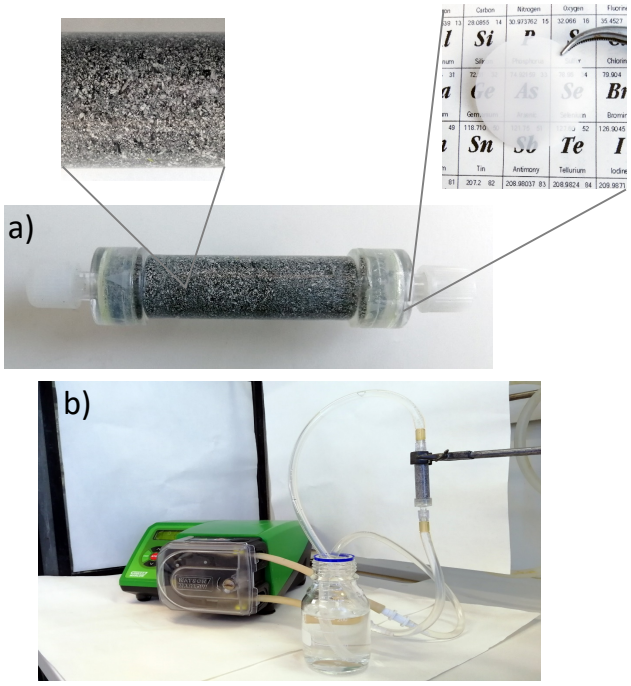

Figure S11. a) A cartridge prototype filled by 1 gr of PSU-GO-OV. The inset shows the material and the nylon disk (cutoff 20 μm) used to stop the material. b) Experimental setup used for studying the possible release of GO sheets from the coating. Water flow is 2 L/h, recirculated for 100 h.

12. Dynamic Light Scattering (DLS)

Detection of GO in liquids is typically performed by spectroscopic techniques; either UV/visible light absorption[14] or Raman spectroscopy.[15] Given our target application, techniques are needed to detect possible release of GO even at very low concentrations; ideally, ppm (≈1mg/L levels). We shall estimate the maximum light absorption of the possible GO traces using Beer-Lambert law:

$A=C\,\varepsilon\,L$, C being the lowest concentration (1 mg/L), L being the optical path length (typically 1 cm) and ε the molar extinction coefficient of GO (3592 ml mg^{-1} m^{-1} from ref. [16]).

DLS was performed by a NanoBrook-Omni. Samples at different concentration of GO in milliQ water were prepared by adding proper amounts of GO suspension from a standard of 1mg/ml sonicated for 2hs before use.

Figure S12 shows the DLS of mQ water (blue lines), of mQ water contaminated with 10 ppm of GO (red lines), of mQ water filtered through cartridge filters containing the PSU-GO composite. Figure S12b shows the particles size distribution of GO in mQ. The intensity of the correlation function is extremely low in mQ water, while the signal on mQ filtered by PSU-GO-OV is higher, but one order of magnitude lower that the water containing 10 ppm of GO.

At 5 ppm of GO the instrument gave a response similar to that of mQ water, i.e. close to the limit of the detection (alerts signal appears during the measurements). This suggest a limit of detection for GO in the concentration range 5-10 ppm. Figure S13 shows the DLS response of tap water (blue lines); GO 10 ppm in TAP water filtered on a cellulose filter 0,45 μm before the analysis (red lines) and tap water filtered through cartridge filters containing the PSU-GO composite (black lines). The intensity of the correlation function for the PSU-GO filtered tap water was of the same order of magnitude of the pure tap water, suggesting negligible presence of GO.

DLS analysis of tap water and tap water filtered on PSU-GO gave an unreliable signal, i.e. close to the limit of detection of the instrument.

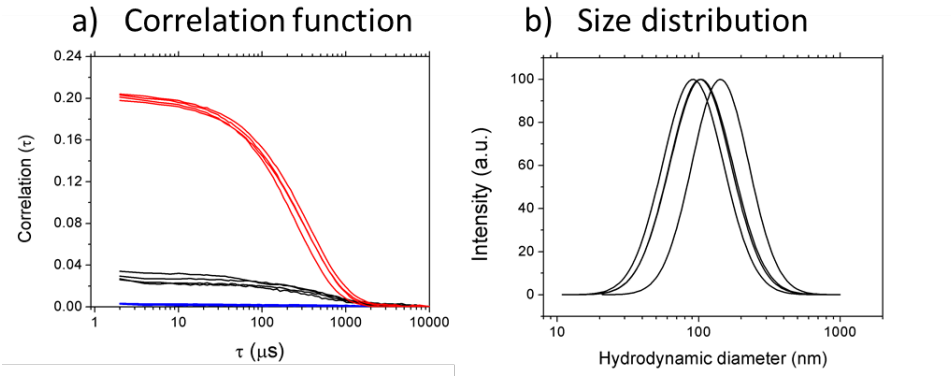

Figure S12. a) DLS of mQ water (blue lines), of mQ water contaminated with 10 ppm of GO (red lines), of mQ water filtered through cartridge filters containing the PSU-GO composite. b) Size distribution of GO nanosheets (10 ppm) in mQ water. Five different independent tests performed for each sample.

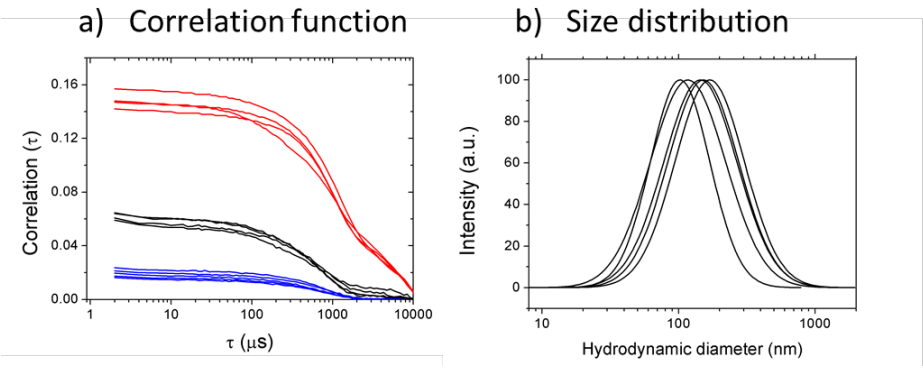

Figure S13. a) DLS of tap water (blue lines); tap water filtered on a PSU-GO-OV cartridge (black lines); GO suspension (10 ppm) in tap water, after filtration with cut-off 0,45 μm (red lines); b) Size distribution of GO nanosheets (10 ppm) in tap water. Five different independent tests performed for each sample.

13. Concentration experiments to enhance the detection limit

We tried to concentrate the sample to further enhance the detection of contaminants, both by ultracentrifugation and vacuum evaporation failed (Figures S14, S15, S16, S17).

We frist tried to concentrate the recirculated water sample by centrifugation at 18000 rpm for 1h. After centrifugation, the solution was still transparent (see Figure S14, ESI). We also centrifuged standard GO solutions with known concentration of 0.1, 1 and 10 ppm in water. After 1 h a precipitate was observed only for the sample at 10 ppm, thus limiting the detection threshold of the method.

We tried to concentrate the solution in a different way, removing water by vacuum evaporation. Abundant salts amount in tap water were observed with UV-vis strong signal in the range 200-250 nm (Figure S16, ESI).

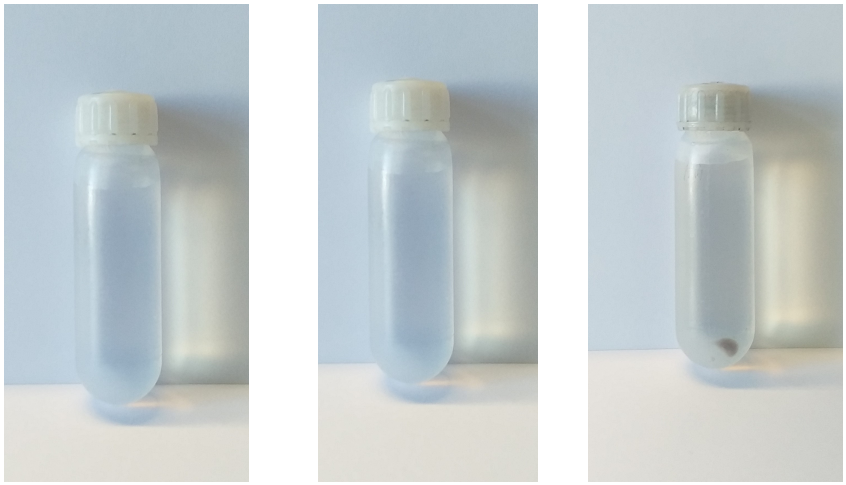

Figure S14. Images of samples of standard of GO in mQ water (total volume 30 ml) at different concentration after centrifugation for 1h at 18000 rpm. No precipitate is observed, thus limiting the use of centrifugation as a way to preconcentrate the water solution.

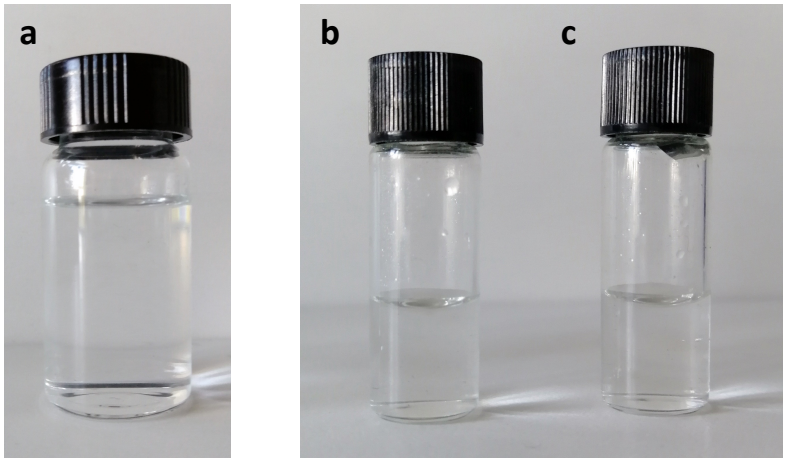

Figure S15. a) recirculated water, b) two samples of recirculated water from two different experiments after concentration of about 100 times.

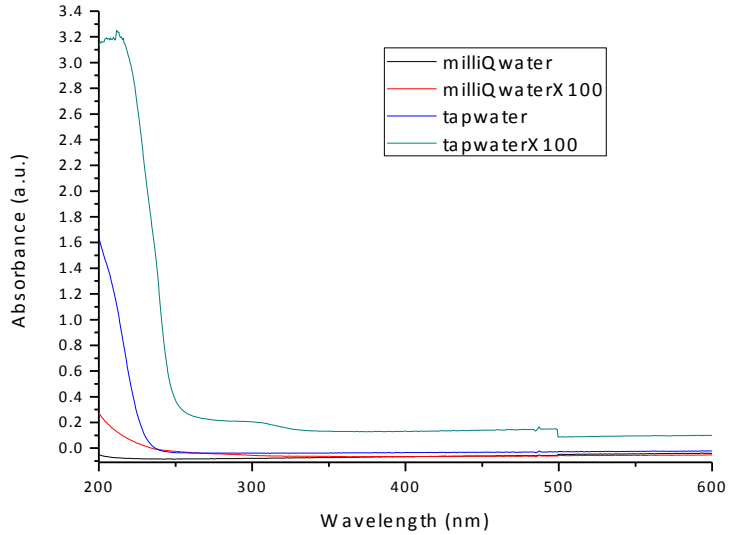

Figure S16. UV-vis spectra of tap water and milliQ water before and after concentration ≈100-fold by evaporation (volume of the solution reduced from 100 ml to 1 ml). After –concentration, the background signal increased due to the intrinsic composition of the matrixes.

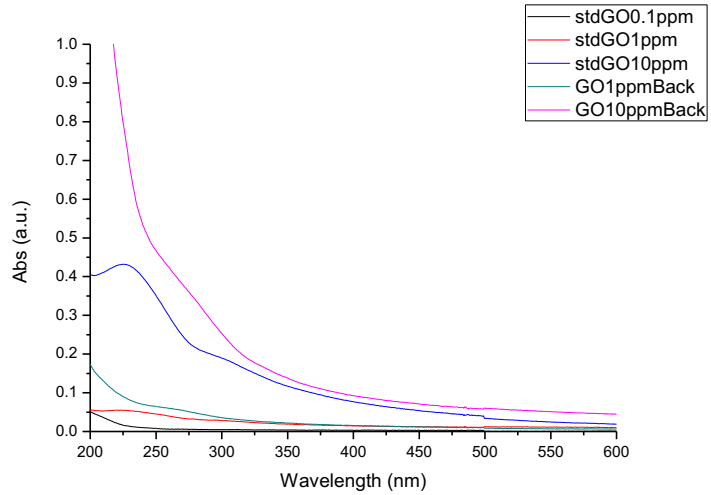

Figure S17. UV-vis spectra of standard solutions of GO in mQ water at different concentration as prepared (stdGO) and after concentration of a factor 100 (GOback).

14. References

[1] E. Treossi, M. Melucci, A. Liscio, M. Gazzano, P. Samorì, and V. Palermo, *High-Contrast Visualization of Graphene Oxide on Dye-Sensitized Glass, Quartz, and Silicon by Fluorescence Quenching.* **Journal of the American Chemical Society**, 131, (2009) 15576.

[2] M. Zambianchi, M. Durso, A. Liscio, E. Treossi, C. Bettini, M.L. Capobianco, A. Aluigi, A. Kovtun, G. Ruani, F. Corticelli, M. Brucale, V. Palermo, M.L. Navacchia, and M. Melucci, *Graphene oxide doped polysulfone membrane adsorbers for the removal of organic contaminants from water.* **Chemical Engineering Journal**, 326, (2017) 130.

[3] M. Melucci, M. Durso, M. Zambianchi, E. Treossi, Z.-Y. Xia, I. Manet, G. Giambastiani, L. Ortolani, V. Morandi, F. De Angelis, and V. Palermo, *Graphene-organic hybrids as processable, tunable platforms for pH-dependent photoemission, obtained by a new modular approach.* **Journal of Materials Chemistry**, 22, (2012) 18237.

[4] M. Melucci, E. Treossi, L. Ortolani, G. Giambastiani, V. Morandi, P. Klar, C. Casiraghi, P. Samori, and V. Palermo, *Facile covalent functionalization of graphene oxide using microwaves: bottom-up development of functional graphitic materials.* **Journal of Materials Chemistry**, 20, (2010) 9052.

[5] A. Liscio, K. Kouroupis-Agalou, X.D. Betriu, A. Kovtun, E. Treossi, N.M. Pugno, G. De Luca, L. Giorgini, and V. Palermo, *Evolution of the size and shape of 2D nanosheets during ultrasonic fragmentation.* **2d Materials**, 4, (2017) #025017.

[6] F. Perrozzi, S. Prezioso, M. Donarelli, F. Bisti, P. De Marco, S. Santucci, M. Nardone, E. Treossi, V. Palermo, and L. Ottaviano, *Use of Optical Contrast To Estimate the Degree of Reduction of Graphene Oxide.* **Journal of Physical Chemistry C**, 117, (2013) 620.

[7] J. Russier, E. Treossi, A. Scarsi, F. Perrozzi, H. Dumortier, L. Ottaviano, M. Meneghetti, V. Palermo, and A. Bianco, *Evidencing the mask effect of graphene oxide: a comparative study on primary human and murine phagocytic cells.* **Nanoscale**, 5, (2013) 11234.

[8] R. Kurapati, J. Russier, M.A. Squillaci, E. Treossi, C. Menard-Moyon, A. Esau Del Rio-Castillo, E. Vazquez, P. Samori, V. Palermo, and A. Bianco, *Dispersibility-Dependent Biodegradation of Graphene Oxide by Myeloperoxidase.* **Small**, 11, (2015) 3985.

[9] M. Zambianchi, A. Aluigi, M.L. Capobianco, F. Corticelli, I. Elmi, S. Zampolli, F. Stante, L. Bocchi, F. Belosi, M.L. Navacchia, and M. Melucci, *Polysulfone Hollow Porous Granules Prepared*

from Wastes of Ultrafiltration Membranes as Sustainable Adsorbent for Water and Air Remediation. **Advanced Sustainable Systems**, 1, (2017) #1700019.

[10] H.P. Klug and L.E. Alexander, *X-ray Diffraction Procedures*. 1974, New York: Wiley.

[11] N.M. Patel, D.W. Dwight, J.L. Hedrick, D.C. Webster, and J.E. McGrath, *SURFACE AND BULK PHASE-SEPARATION IN BLOCK COPOLYMERS AND THEIR BLENDS - POLYSULFONE POLYSILOXANE.* **Macromolecules**, 21, (1988) 2689.

[12] A. Kovtun, D. Jones, S. Dell'Elce, E. Treossi, A. Liscio, and V. Palermo, Accurate chemical analysis of oxygenated graphene-based materials using X-ray photoelectron spectroscopy. **Carbon**, 143, (2019) 268.

[13] A. Ebadi, J.S.S. Mohammadzadeh, and A. Khudiev, *What is the correct form of BET isotherm for modeling liquid phase adsorption?* **Adsorption-Journal of the International Adsorption Society**, 15, (2009) 65.

[14] Y. Hernandez, V. Nicolosi, M. Lotya, F.M. Blighe, Z.Y. Sun, S. De, I.T. McGovern, B. Holland, M. Byrne, Y.K. Gun'ko, J.J. Boland, P. Niraj, G. Duesberg, S. Krishnamurthy, R. Goodhue, J. Hutchison, V. Scardaci, A.C. Ferrari, and J.N. Coleman, *High-yield production of graphene by liquid-phase exfoliation of graphite.* **Nature Nanotechnology**, 3, (2008) 563.

[15] A.C. Ferrari, Raman spectroscopy of graphene and graphite: Disorder, electron-phonon coupling, doping and nonadiabatic effects. **Solid State Communications**, 143, (2007) 47.

[16] D. Konios, M.M. Stylianakis, E. Stratakis, and E. Kymakis, *Dispersion behaviour of graphene oxide and reduced graphene oxide.* **Journal of Colloid and Interface Science**, 430, (2014) 108.